PII: S0955-2219(97)00077-0

Growth of AlN, GaN and Al$_x$Ga$_{1-x}$N Thin Films on Vicinal and On-axis 6H-SiC(0 0 0 1) Substrates

Robert F. Davis, M. D. Bremser, W. G. Perry and K. S. Ailey

Department of Materials Science and Engineering, Box 7907, North Carolina State University, Raleigh, NC 27695-7907, USA

Abstract

Monocrystalline GaN(0 0 0 1) thin films were grown at 950°C on AlN(0 0 0 1) buffer layers previously deposited at 1100°C on α(6H)-SiC(0 0 0 1)$_{Si}$ substrates via metallorganic chemical vapor deposition (MOCVD). Films of Al$_x$Ga$_{1-x}$N (0 ≤ x ≤ 1) were grown directly on the same SiC surface at 1100°C. X-ray rocking curves for the GaN(0 0 0 4) reflection for 1·4 μm films revealed FWHM values of 58 and 151 arc sec for materials grown on on-axis and off-axis substrates, respectively. Cathodoluminescence exhibited strong near band-edge emission for all materials. Controlled n- type Si-doping in GaN and Al$_x$Ga$_{1-x}$N (for x ≤ 0·4) was achieved with net carrier concentrations ranging from approximately 2 × 10^{17} cm^{-3} to 2 × 10^{19} (Al$_x$Ga$_{1-x}$N) or to 1 × 10^{20} (GaN) cm^{-3}. Mg-doped, p-type GaN and Al$_x$Ga$_{1-x}$N (for x ≤ 0·13) was achieved with n$_A$−n$_D$ ≈ 3 × 10^{17} cm^{-3}. © 1997 Elsevier Science Limited.

1 Introduction

The numerous potential semiconductor applications of the wide bandgap III-Nitrides has prompted significant research regarding their growth and development. GaN (wurtzite structure), the most studied in this group, has a bandgap of ≈3·4 eV and forms continuous solid solutions with both AlN (6·2 eV) and InN (1·9 eV). As such, materials with engineered bandgaps are feasible for optoelectronic devices tunable in wavelength from the visible to the deep UV. The relatively strong atomic bonding of these materials also points to their application for high-power and high-temperature microelectronic devices. Diodes emitting light from the yellow into the blue regions of the spectrum, blue emitting lasers, and several types of high frequency and high power devices have recently been fabricated from these materials.

Single crystal wafers of GaN are not commercially available. Sapphire (0 0 0 1) is the most commonly used substrate, although its lattice parameter and coefficients of thermal expansion are significantly different from that of any III-Nitride. The heteroepitaxial nucleation and growth of monocrystalline films of GaN on any substrate and AlN on sapphire are difficult at elevated (>900°C) temperatures. Therefore, at present, for successful organometallic vapor phase epitaxy (OMVPE) of GaN films on sapphire the use of the initial deposition of an amorphous or polycrystalline buffer layer of AlN[1,2] or GaN[3,4] at low temperatures (450–600°C) is necessary to achieve both nucleation an relatively uniform coverage of the substrate surface. Subsequent deposition at higher temperatures and concomitant grain orientation competition has resulted in films of GaN(0 0 0 1) and various nitrides alloys of improved quality and surface morphology relative to that achieved by growth directly on this substrate.

By contrast, we have observed that AlN and Al$_x$Ga$_{1-x}$N alloys containing even low (x ≥ 0·05) concentrations of AlN deposited on 6H-SiC(0 0 0 1) substrates at high (≥ 1000°C) temperatures undergo two-dimensional nucleation and growth with resulting uniform surface coverage. In this research, the use of a 1000 Å, monocrystalline, high-temperature (1100°C) AlN buffer has resulted in GaN films void of oriented domain structures and associated low-angle grain boundaries.[5,6] Monocrystalline films of Al$_x$Ga$_{1-x}$N (0·05 ≤ x ≤ 0·70) of the same quality have also been achieved at 1100°C.

The investigations up to 1975 regarding III-Nitrides in terms of thin film growth, characterization, properties and device development have been reviewed by Kesamanly[7] and Pankove and Bloom[8]. The considerable progress accomplished in these areas in the intervening years has been reviewed in Refs. [9-16] Research in the authors' group at NCSU employs both MOCVD and GSMBE to grow GaN and $Al_xGa_{1-x}N$ films on α(6H)-SiC(0 0 0 1)$_{Si}$ substrates. Only the investigations involving the former technique are described herein.

In the present research, GaN and $Al_xGa_{1-x}N$ films were deposited either on monocrystalline high-temperature (HT) AlN buffer layers previously deposited on vicinal and on-axis 6H-SiC(0 0 0 1) substrates (GaN) or directly on the SiC ($Al_xGa_{1-x}N$ alloys). The n- and p-type doping of GaN and $Al_xGa_{1-x}N$ using Si and Mg dopants, respectively, has also been accomplished. Extensive chemical, optical, microstructural and electrical characterization of the binary and ternary films has also been conducted. The following sections describe the experimental procedures and results and provide a discussion and conclusions regarding this research.

2 Experimental Procedures

As-received vicinal (oriented 3°–4° off-axis toward $<1 1 \bar{2} 0>$) and on-axis 6H-SiC(0 0 0 1)$_{Si}$ wafers containing an $\approx 1\,\mu$m n-type homoepitaxial layer which had been thermally oxidized were cut into 7·1 mm squares, degreased in sequential ultrasonic baths of trichloroethylene, acetone and methanol and rinsed in deionized water. They were subsequently dipped into a 10% HF solution for 10 min to remove the thermally grown oxide layer and blown dry with N_2 before being loaded onto a SiC-coated graphite susceptor contained in a cold-wall, vertical, pancake-style reactor. The diffusion-pumped system was evacuated to less than 3×10^{-5} Torr prior to initiating growth. The continuously rotating susceptor was RF inductively heated to the AlN or $Al_xGa_{1-x}N$ deposition temperature of 1100°C (as measured optically on the susceptor) in 3 SLM of flowing H_2 diluent. Hydrogen was also used as the carrier gas for the various metalorganic reactants and dopants. Deposition of each AlN buffer layer or $Al_xGa_{1-x}N$ was initiated by flowing triethylaluminum (TEA), triethylgallium (TEG) and ammonia (NH_3) into the reactor at 23·6–32·8 μmol min^{-1} (total MO flow rate) and 1·5 SLM, respectively. The system pressure during growth was 45 Torr. Each AlN buffer layer was grown for 30 min resulting in a thickness of ≈ 100 nm. The TEA flow was subsequently termi-

nated, the susceptor temperature decreased to 950°C and the system pressure increased to 90 Torr for the GaN growth. The flow rate of triethylgallium (TEG) was maintained at 24·8 μmol min^{-1}. The growth rate for GaN was $\approx 0.9\,\mu$m h^{-1}. Silicon-doped GaN and $Al_xGa_{1-x}N$ films were grown by additionally flowing SiH_4 (8·2–12·4 ppm in a balance of N_2) at flow rates between ≈ 0.05 nmol min^{-1} and ≈ 15 nmol min^{-1}. Mg-doping of GaN was accomplished by introducing bis-cyclopentadienylmagnesium (Cp_2Mg) at a flow rate of 0·2 μmol min^{-1}.

The structural, microstructural, optical and electrical characteristics of the epitaxial films were analyzed using transmission and scanning electron microscopies, double-crystal X-ray rocking curve (DCXRC) measurements of the GaN(0 0 0 4) and AlN(0 0 0 2) reflections, photoluminescence (PL) and cathodoluminescence (CL) at 8K using a 15 m W He-Cd laser ($\lambda = 325$ nm) or electron gun operated at 6 keV and a beam current of $100\,\mu$A as the respective excitation sources. Secondary ion mass spectrometry of the dopants was accomplished using a Cameca ims-3f. The carrier concentrations and mobilities in the Si- and Mg-doped GaN and the Si-doped $Al_xGa_{1-x}N$ films were determined via Hall-effect measurements (Van der Pauw geometry). Thermally evaporated Al (GaN) and In ($Al_xGa_{1-x}N$) served as the ohmic contacts. Capacitance-voltage (CV) measurements were also conducted on the Mg-doped GaN and the Si-doped $Al_xGa_{1-x}N$ using an Hg probe. Separately deposited AlN buffer layers were characterized using reflection high-energy electron diffraction (RHEED) and SEM.

3 Results and Discussion

3.1 AlN and GaN

The AlN films grown on the vicinal and on-axis 6H-SiC(0 0 0 1)$_{Si}$ substrates were monocrystalline, as determined via RHEED analysis, with a smooth surface morphology. Coalescence of GaN islands occurred on monocrystalline HT-AlN buffer layers on vicinal and on-axis 6H-SiC(0 0 0 1)$_{Si}$ substrates within the first several hundred angstroms of growth. The SEM image in Fig. 1 shows an intermediate stage of coalescence of ≈ 150 Å thick GaN islands after 1 min of growth. Subsequent growth occurred by a layer-by-layer mechanism. By contrast, for GaN film growth on low-temperature buffer layers on sapphire(0 0 0 1) a similar growth scenario pertains but requires several thousand angstroms of deposition and crystallographic geometric selection before island coalescence and layer-by-layer growth result.[17,18]

Fig. 1. SEM image showing an intermediate stage of coalescence of ≈ 150 Å thick GaN islands after 1 min of growth on a monocrystalline AlN buffer layer deposited at 1100°C on a 6H-SiC(0 0 0 1)$_{Si}$ substrate.

The monocrystalline GaN films deposited on the HT-AlN buffer layers on the on-axis 6H-SiC(0 0 0 1)$_{Si}$ substrates had very smooth surfaces. A slightly mottled surface was observed for films deposited on vicinal 6H-SiC(0 0 0 1)$_{Si}$ substrates, probably as a result of the higher density of steps coupled with the mismatch in the Si/C and Al/N bilayer stacking sequences at selected steps[19] on the growth surface of the this substrate. A representative cross-sectional TEM micrograph of such a film is shown in Fig. 2. No low-angle grain boundaries, twins or stacking faults were observed in these images. Residual lattice strain resulting from inversion domain boundaries (IDBs) generated at the SiC steps as a result of the difference in the Si/C and Al/N bilayer stacking sequence[19] along (0 0 0 1) and resultant threading dislocations were apparent

in the AlN buffer layers. The dislocation density within the first 0·5 μm of the GaN film on the vicinal 6H-SiC(0 0 0 1)$_{Si}$ substrate was approximately 1×10^9 cm^{-2}, as determined from initial plan view TEM analysis by counting the number of dislocations per unit area. This value is approximately an order of magnitude lower than that reported[20] for thicker GaN films deposited on sapphire (0 0 0 1) substrates using low-temperature buffer layers. The dislocation density of the GaN film deposited on the vicinal 6H-SiC(0 0 0 1)$_{Si}$ substrate decreased rapidly as a function of thickness. The on-axis wafers had less step and terrace features; thus, the HT-AlN buffer layers on these substrates were of higher microstructural quality with smoother surfaces and fewer IDBs. Consequently, the microstructural quality of the GaN films were better for on-axis growth as shown by the DCXRC data noted below.

Measurements taken via DCXRC on simultaneously deposited 1·4 μm GaN films on HT-AlN (1100°C) buffer layers revealed full width at half maximum (FWHM) values to be 58 arc sec and 151 arc sec for deposition on the on-axis and off-axis 6H-SiC(0 0 0 1)$_{Si}$ substrates, respectively. The FWHM values of the DCXRC values for the corresponding 100 nm AlN buffer layers were approximately 200 and 400 arc sec. These latter values were unchanged by increasing the growth temperature to 1200°C. The 2·7 μm GaN film deposited under identical conditions on a vicinal 6H-SiC(0 0 0 1)$_{Si}$ substrate yielded a FWHM value of 66 arc sec. The reduction in FWHM values is consistent with the decrease in the dislocation density as a function of thickness for GaN films grown on vicinal 6H-SiC(0 0 0 1)$_{Si}$ substrates, as noted above.

The low-temperature (8K) PL spectra of the GaN films on both on-axis and vicinal 6H-SiC(0 0 0 1)$_{Si}$ substrates showed strong near band-edge emission at 357·4 nm (3·47 eV). The FWHM values of these I_2 bound exciton peaks were 4 meV. The spectra for all the films revealed a very weak peak centered at ≈ 545 nm (2·2 eV), commonly associated with deep levels (DL) in the band gap.

Undoped high quality GaN films grown on HT-AlN buffer layers on both vicinal and on-axis 6H-SiC(0 0 0 1)$_{Si}$ substrates were too resistive for Hall-effect measurements. Controlled n-type doping was achieved using SiH$_4$ for net carrier concentrations ranging from $\approx 1 \times 10^{17}$ cm^{-3} to $\approx 1 \times 10^{20}$ cm^{-3} in GaN films grown on vicinal 6H-SiC(0 0 0 1)$_{Si}$ substrates. The net carrier concentrations and room temperature mobilities versus SiH4 iow rate are plotted in Fig. 3.

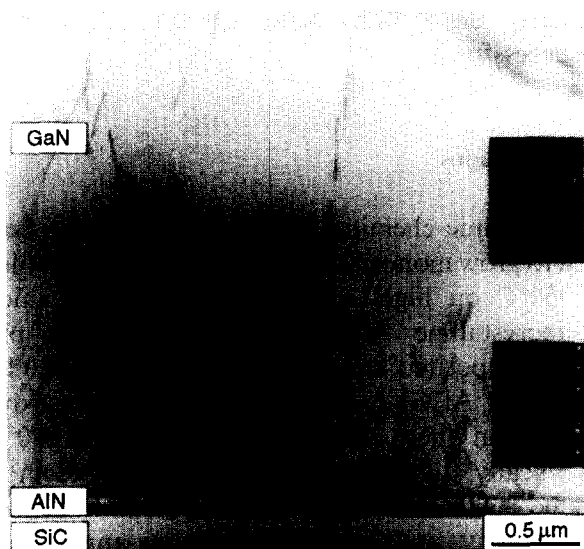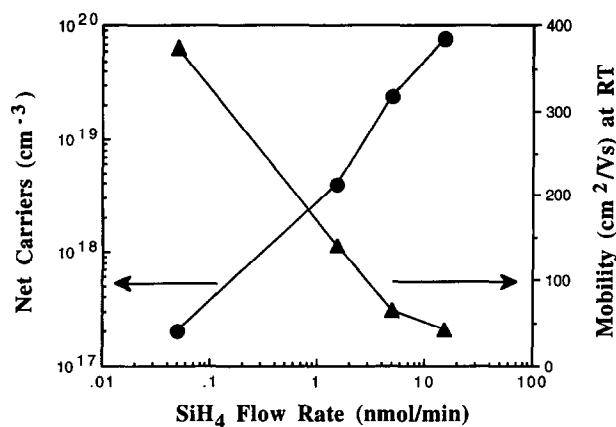Mg-doped GaN films were deposited at 950°C on HT-AlN (1100°C) buffer layers on vicinal

Fig. 2. Cross-sectional TEM micrograph of GaN grown at 950°C on a monocrystalline AlN buffer layer deposited at 1100°C on a vicinal 6H-SiC(0 0 0 1)$_{Si}$ substrate.

Fig. 3. Net carrier concentration and room temperature mobilities in Si-doped, n-type GaN as a function of SiH$_4$ flow rate.

Fig. 4. DCXRC FWHM values versus alloy concentration for Al$_x$Ga$_{1-x}$N films simultaneously deposited on vicinal and on-axis 6H-SiC(0 0 0 1) substrates.

6H-SiC(0 0 0 1)$_{Si}$ substrates which were subsequently annealed at 700°C at 700 Torr in 3 SLM of N$_2$ for 20 min. These same samples were re-annealed at 900°C for 20 min under identical conditions. Similar to the results of Nakamura et al.,[21] the PL intensity of the blue emission was increased by the 700°C anneal and was dramatically decreased by the subsequent 900°C anneal. Hall-effect measurements made on the annealed samples revealed p-type GaN with a net hole carrier concentration of n_A-n_D ≈ 3×10^{17} cm^{-3}, a resistivity of $\rho \approx$ Ω·cm and a hole mobility of $\mu \approx$ 3 cm^2 V·s^{-1}. Likewise, 4-point probe and Hg-probe C-V measurements verified p-type GaN.

3.2 Al$_x$Ga$_{1-x}$N

Al$_x$Ga$_{1-x}$N films have been grown for Al mole fractions of $0 \leq x \leq 1$. Al$_x$Ga$_{1-x}$N films for $0 < x < 0.3$ were then simultaneously deposited directly on vicinal and on-axis 6H-SiC(0 0 0 1) substrates without the use of the customary high-temperature AlN buffer layers. These films were electrically insulating as-grown. The Al mole fractions were determined by low-temperature CL measurements as described below. The DCXRC measurements again revealed smaller FWHM values for Al$_x$Ga$_{1-x}$N films grown on the on-axis substrates as compared to simultaneously deposited films grown on vicinal substrates. Also, the FWHM values expand with increasing Al mole fraction. These results are shown in Fig. 4.

The low-temperature (8K) CL spectra of the Al$_x$Ga$_{1-x}$N films with $x < 0.5$ showed strong near band-edge emission. As expected, the energy positions of these peaks shifted towards higher energy with increasing x. The Al mole fractions were assigned from the near band-edge peak positions using a bowing parameter of b = 0.98 eV, as determined by Khan et al.[22]
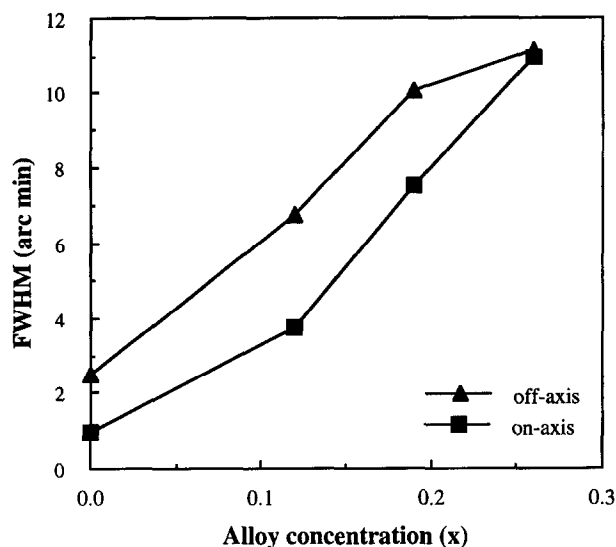
The FWHM of the energy peaks increased with increasing values of x. Al$_x$Ga$_{1-x}$N films grown on the on-axis substrates showed a similar trend. The broadening of the near band-edge peak is possibly due to increased fluctuations in the alloy compositions of Al$_x$Ga$_{1-x}$N films for increasing values of x.[22] The CL peak intensities were 0.1 to 1 order of magnitude stronger for undoped AlGaN films grown on vicinal substrates than for films grown on the on-axis substrates. This phenomenon is being further investigated.

The controlled introduction of SiH$_4$ allowed the reproducible achievement of donor carrier concentrations within the range of 2×10^{17} cm^{-3} to 2×10^{19} cm^{-3} in films with $x \leq 0.4$. The growth of p-type Al$_x$Ga$_{1-x}$N films for $x \leq 0.13$ via the introduction of Mg has been successful. All attempts to similarly dope films with $x > 0.13$ have been unsuccessful.

4 Conclusions

Metalorganic chemical vapor deposition has been used to grow monocrystalline GaN(0 0 0 1) thin films at 950°C on high-temperature on 100 nm thick, monocrystalline AlN(0 0 0 1) buffer layers previously deposited at 1100°C on α(6H)-SiC(0 0 0 1)$_{Si}$ substrates. Al$_x$Ga$_{1-x}$N films ($0 \leq x \leq 1$) were grown directly on these substrates at 1050 or 1100°C. Chemically abrupt heterojunctions were demonstrated. All films possessed a smooth surface morphology and were free of low-angle grain boundaries and associated oriented domain microstructures. The PL spectra of the GaN films deposited on both vicinal and on-axis substrates

revealed strong bound exciton emission with a FWHM value of 4 meV. The spectra of these films on the vicinal substrates were shifted to a lower energy, indicative of films containing residual tensile stresses. A peak believed to be associated with free excitonic emission was also observed in each on-axis spectrum. Cathodoluminescence of solutions with x < 0·5 exhibited strong near band-edge emission with a FWHM as low as 31 meV. The CL spectra of the Al$_x$Ga$_{1-x}$N films for x < 0·5 showed strong near band-edge emission. The FWHM values of the main energy peak increased with increasing Al mole fraction. Controlled n- type Si-doping in GaN and Al$_x$Ga$_{1-x}$N (for x ≤ 0·4) was achieved for net carrier concentrations ranging from approximately 2×10^{17} cm^{-3} to 2×10^{19} (Al$_x$Ga$_{1-x}$N) or to 1×10^{20} (GaN) cm^{-3}. Mg-doped, p-type GaN was achieved with n_A-n_D ≈ 3×10^{17} cm^{-3}, ρ ≈ 7Ω·cm and μ ≈ 3 cm^2 V·s^{-1}.

Acknowledgements

References

1. Khan, M. A., Kuznia, J. N., Olson, D. T. and Kaplan, R., *J. Appl. Phys.*, 1993, **73**, 3108.
2. Amano, H., Akasaki, I., Hiramatsu, K., Koide, N. and Sawaki, N., *Thin Solid Films*, 1988, **163**, 415.
3. Kuznia, J. N., Khan, M. A., Olson, D. T., Kaplan, R. and Freitas, J., *J. Appl. Phys.*, 1993, **73**, 4700.
4. Nakamura, S., Jpn. *J. Appl. Phys.*, 1991, **30**, L1705.
5. Weeks, Jr., T. W., Bremser, M. D., Ailey, K. S., Carlson, E. P., Perry, W. G. and Davis, R. F., *Appl. Phys. Lett.*, 1995, **67**, 401.
6. Weeks Jr., T. W., Bremser, M. D., Ailey, K. S., Perry, W. G., Carlson, E. P., Piner, E. L., El-Masry, N. A. and Davis, R. F., *J. Mat. Res.*, 1996, **11**, 1081.
7. Kesamanly, F. P., *Sov. Phys. Semicond.* 1974, **8**, 147.
8. Pankove, J. I. and Bloom, S., *RCA Rev.*, 1975, **36**, 163.
9. Davis, R. F. *et al.*, *J. Mater. Sci. Eng.*, 1988, **B1**, 77.
10. Strite, S. and Morkoc, H., *J. Vac. Sci. Technol. B*, 1992 **10**, 1237.
11. Pankove, J. I., In *Diamond, silicon carbide and related wide bandgap semiconductor materials*. In *Mater. Res. Soc. Sym Proc*, Vol. 116, eds. J. T. Glass, R. F. Messier and N. Fujimori, Pittsburgh, PA, 1990, pp. 515–524.
12. Davis, R. F., *Proc. IEEE*, 1991, **79**, 702.
13. Morkoç, H., *J. Appl. Phys.*, 1994, **76**, 1363.
14. Edgar, J. H., *J. Mater. Res.*, 1992, 7, 235.
15. Henin, M., *Microelectron J*, 1992, **23**, 500.
16. Morkoç, H., Strite, S., Gao, G. B., Lin, M. E., Sverdlov, B. and Burns, M., *J. Appl Phys.*, 1994, **76**, 1363.
17. Akasaki, I., Amano, H., Koide, N. Hiramatsu K. and Sawaki, N. N., *J. Cryst. Growth*, 1989, **98**, 209.
18. Hiramatsu, K., Itoh, S., Amano, H., Akasaki, I., Koide, N. H. and Sawaki, N. N., Kuwano, N., Shiraishi, T. and Oki, K. *J. Crystal Growth*, 1991, **115**, 628.
19. Tanaka, S., Kern, R. S. and Davis, R. F., *Appl. Phys. Lett.*, 1995, **66**, 37.
20. Qian, W., Skowronski, M., De Graef, M., Doverspike, K., Rowland, L. B. and Gaskill, D. K., *Appl. Phys. Lett.*, 1995, **66**, 1252.
21. Nakamura, S., Iwasa, N., Senoh, M. and Mukai, T., *Jpn. J. Appl. Phys.*, 1992, **31**, 1258.
22. Khan, M. R. H., Koide, N. H., Sawaki, N. and Akasaki, I., *Solid State Commun.*, 1986, **60**, 509.